European Journal of Radiology 187 (2025) 112079

Contents lists available at ScienceDirect

European Journal of Radiology

journal homepage: www.elsevier.com/locate/ejrad

Research article

The Node Reporting and Data System (Node-RADS) for standardized MRI evaluation of lymph nodes in endometrial cancer, integrated with clinicopathological and molecular data

Sandrine Riccardi [a,1], Roberta Valerieva Ninkova [b,1], Alessandro Calabrese [a], Federica Curti [a], Marco Gennarini [a], Valentina Miceli [a], Angelica Cupertino [a], Claudia Cutonilli [a], Violante Di Donato [c], Angelina Pernazza [a], Stefania Maria Rita Rizzo [d], Valeria Panebianco [a], Carlo Catalano [a], Lucia Manganaro [a,*]

[a] Department of Radiological, Oncological and Pathological Sciences, Sapienza University of Rome, Policlinico Umberto I, Viale del Policlinico 155, 00161 Rome, Italy
[b] Department of Experimental Medicine, Sapienza - University of Rome, Viale Regina Elena, 324, 00161 Rome, Italy
[c] Department of Maternal and Child Health and Urological Sciences, Oncological and Pathological Sciences, Sapienza, University of Rome, Policlinico Umberto I, Viale del Policlinico 155, 00161 Rome, Italy
[d] Service of Radiology, Imaging Institute of Southern Switzerland, Ente Ospedaliero Cantonale (EOC), 6500 Lugano, Switzerland

A B S T R A C T

Objectives: To evaluate the diagnostic performance of Node-RADS score using magnetic resonance imaging (MRI) in predicting lymph node involvement (LNI) in patients with endometrial cancer (EC). Additionally, the applicability of the Node-RADS score was evaluated by three readers with different levels of experience in pelvic imaging. Finally, this study investigated the correlation between the Node-RADS score and the extent of myometrial invasion, histological type, lympho vascular invasion (LVI) and molecular subtype.

Methods: Out of 108 cases, 82 patients with histologically confirmed locally advanced EC met the inclusion criteria for retrospective analysis. LNI risk was assessed for each pelvic lymph node station using a Node-RADS score (1–5). Diagnostic accuracy was determined by comparing scores to histologic findings, considered as the gold standard. Three independent readers with different experience levels assigned scores.

Results: The Node-RADS score strongly correlated with histologically confirmed LNI (AUC: 0.832). A cutoff of Node-RADS ≥ 3 optimally detected metastatic lymph nodes, with 85.71 % sensitivity and 76.47 % specificity. Interobserver agreement was high, with κ values of 0.86 (senior vs. junior reader 1) and 0.70 (senior vs. junior reader 2). A significant positive correlation was found between Node-RADS score and myometrial invasion as well as LVI.

Conclusion: Node-RADS score is a reliable, standardized tool for assessing LN stations and enhancing diagnostic accuracy in locoregional staging of EC.

1. Introduction

Endometrial cancer (EC) is the most prevalent form of gynecological cancer and the 6th most common cancer in women, with 420,368 new cases reported worldwide in 2022[1]. It predominantly affects post-menopausal women, with a median age at diagnosis of 61 years[2]. In 2023, the International Federation of Gynecology and Obstetrics (FIGO) revised the staging system for EC, incorporating histopathological subtypes, tumor patterns, and molecular classifications[3].

In the updated classification, histological subtypes of EC are stratified into aggressive and non-aggressive categories. The Cancer Genome Atlas (TCGA) also defines and stratifies EC into four molecular classes: polymerase epsilon mutations (POLEmut) associated clinically with a favorable prognosis; mismatch repair deficiency/microsatellite instability (MMRd/msi), no specific molecular profile (NSMP) indicative of intermediate prognosis, and abnormal p53 (p53abn), which correlates with a poor prognosis. In fact, this classification can refine staging for stage I-II EC, particularly a POLEmut EC is classified as Stage

* Corresponding author.
E-mail addresses: sandrine.riccardi@uniroma1.it (S. Riccardi), robertavalerieva.ninkova@uniroma1.it (R.V. Ninkova), alessandro.calabrese.92@gmail.com (A. Calabrese), federica.curti@uniroma1.it (F. Curti), marco.gennarini@uniroma1.it (M. Gennarini), valentina.miceli@uniroma1.it (V. Miceli), angelica.cupertino@uniroma1.it (A. Cupertino), claudia.cutonilli@uniroma1.it (C. Cutonilli), violante.didonato@uniroma1.it (V. Di Donato), angelina.pernazza@uniroma1.it (A. Pernazza), stefania.rizzo@eoc.ch (S.M.R. Rizzo), valeria.panebianco@uniroma1.it (V. Panebianco), carlo.catalano@uniroma1.it (C. Catalano), lucia.manganaro@uniroma1.it (L. Manganaro).
[1] Sandrine Riccardi and Roberta Valerieva Ninkova have contributed equally to this study and should be considered as co-first authors.

https://doi.org/10.1016/j.ejrad.2025.112079
Received 22 January 2025; Received in revised form 13 March 2025; Accepted 26 March 2025
Available online 29 March 2025

IAmPOLEmut, while p53abn EC is classified as Stage IICmp53abn.

Key staging factors remain myometrial invasion, cervical stroma invasion, substantial lymphovascular space invasion (LVSI), and lymph node involvement (LNI).

Traditionally, lymphadenectomy has been used to assess LNI in EC. However, this procedure is associated with significant morbidity and potential complications. Consequently, non-invasive and reliable methods for evaluating LNI are highly desirable to enhance patient outcomes and reduce unnecessary surgical interventions. Sentinel lymph node biopsy (SLNB) has emerged as an alternative to lymph node (LN) dissection for LN staging. When performed following best-practice guidelines, a negative sentinel node is considered sufficient to confirm pN0 status[4].

Magnetic Resonance Imaging (MRI) plays a crucial role in staging EC, particularly in assessing myometrial and cervical stroma invasion, as well as detecting LNI[5]. However, the criteria used to define LNI in radiological reports are not standardized, and may not be easily interpretated by clinicians, complicating treatment decisions, especially when determining whether to perform lymphadenectomy.

In the literature, we found conflicting results regarding the size cutoffs for pelvic LN. The European Society of Urogenital Radiology (ESUR) guidelines suggest a size cutoff of $>$ 8 mm (short axis) for suspicious obturator and internal/external iliac LN and $>$ 10 mm (short axis) for common iliac LN [6]. On the other hand, Elsholtz et al. introduced the Node Reporting and Data System (Node-RADS) score proposing a size cutoff of $>$ 5 mm (short axis) for suspicious obturator and $>$ 10 mm (short axis) internal/external iliac LN and common iliac LN [7]. For this article, we based our analysis on the data from Node-RADS. It combines both size and configuration criteria, to standardize the radiological assessment of LNI. Node-RADS provides a structured and repeatable reporting system, evaluating the likelihood of cancer involvement based on criteria such as nodal size, texture, border, and shape. The results are categorized into five risk levels for malignant nodal involvement[7]. Although Node-RADS has been validated in prostate, cervical, bladder, colon and rectal cancer, its applicability to EC has not yet been investigated [8–12].

If validated for EC, the Node-RADS system could enhance the accuracy and reproducibility of LN assessment, providing clinicians with a standardized and more easily interpretable radiological report. Precise LN evaluation is essential in EC to determine disease extent, directly influencing surgical strategies, adjuvant therapy decisions, and overall prognosis.

The primary aim of this study is to assess the effectiveness of the Node-RADS score in detecting LNI in patients with EC. By comparing Node-RADS scores with histopathological findings, the study aims to determine diagnostic performance (accuracy, sensitivity, specificity, positive predictive value (PPV), and negative predictive value (NPV)) and applicability among radiologists with different levels of experience. Additionally, the correlation between the Node-RADS score and the extent of myometrial invasion, histological type (aggressive or non-aggressive), LVI and molecular subtype was investigated. The findings could pave the way for more effective and less invasive staging strategies for EC, improving patient treatment and outcomes.

2. Material and methods

2.1. Study design and patient population

This retrospective, single-center study was conducted at Policlinico Umberto I – Sapienza University of Rome, Italy, between September 2018 and May 2024. From our institutional database of 346 patients diagnosed with EC, we selected 108 patients who underwent preoperative pelvic MRI and surgery. The preoperative MRI was performed within three weeks prior to surgery.

Although preoperative MRI is not mandatory, the ESUR guidelines recommend its use for accurate preoperative staging. Therefore, patients underwent preoperative MRI whenever possible[13].

This study was performed according to the principles of the Declaration of Helsinki, and informed consent was obtained from all participants included in this study.

Inclusion criteria were patients who had a preoperative pelvic MRI scan with contrast agent, a confirmed histological diagnosis of EC, a complete molecular profile, and a comprehensive anatomopathological report after surgery. Exclusion criteria were patients who underwent only a postoperative pelvic MRI, patients lacking a histological diagnosis of EC with incomplete or partial molecular profiles, patients with prior preoperative therapy, and those with concurrent or previous malignancies [Fig. 1].

All cases have been restaged based on the 2023 revision of the FIGO staging system for EC.

2.2. Surgical management and anatomopathological analysis

Surgical management was performed according to the European Society of Gynaecological Oncology (ESGO), the European Society for Radiotherapy and Oncology (ESTRO), and the European Society of Pathology (ESP) guidelines for the management of patients with EC 2020 [14].

All patients in this study underwent total hysterectomy with bilateral salpingo-oophorectomy using either a laparoscopic or robotic surgical approach. Bilateral sentinel lymph node (SLN) mapping was performed. If SLN mapping failed, systematic lymphadenectomy was performed on the side where mapping failed. Selective pelvic and *para*-aortic lymphadenectomy was conducted in cases of bulky nodal lesions. In cases of suspected advanced disease or high-risk histotypes, peritoneal biopsy and cytology were also performed.

Post-surgical histopathologic type, grade, myometrial invasion, and LVSI, were analyzed on all EC surgical specimens as reported in Table 1 [Table 1]. Additionally, immunohistochemical analysis for markers (p53, MSH6, and PMS2) and molecular testing (mutation analysis of the exonuclease domain of POLE) were performed to delineate prognostic subgroups consistent with the TCGA molecular classification.

2.3. MRI technique

MRI exams were performed using a 3 Tesla (3 T) magnet (either the GE Discovery 750 or Siemens VIDA), with a 32-channel or 16-channel phased-array coil positioned over the lower abdomen to optimize the signal-to-noise ratio and anatomical coverage.

Patients were instructed to fast for 6 h before the exam and to empty their bladder one hour before the scan to ensure optimal bladder distention. To minimize bowel movement artifacts, an intravenous dose of 20 mg scopolamine-N-butylbromide (Buscopan; Boehringer Ingelheim, Germany) was administered to all patients before the exam, unless contraindicated.

The MRI protocol for staging EC followed the updated guidelines from the ESUR [13,5,15].

The study of the pelvis covers from the pubic symphysis to the iliac crests. MRI examinations were performed including the following sequences: T2-weighted fast spin-echo (FSE) with 3 mm slices for enhanced anatomical detail, acquired in sagittal, axial, *para*-axial, and *para*-coronal planes; T1-weighted FSE and fat-saturated T1-weighted images in the axial plane; axial and *para*-axial diffusion-weighted images (DWI) with diffusion-sensitizing gradients using a b-value of 0–1000 s/mm^2, generating apparent diffusion coefficient (ADC) maps, which were processed on a workstation (AW Volume-Share 7, GE Healthcare, Milwaukee, WI, USA); and dynamic T1-weighted 3D gradient-echo sequences with fat saturation during contrast uptake, followed by delayed post-contrast T1-weighted 3D gradient-echo sequences with fat saturation in the axial plane.

A gadolinium-based contrast agent (gadoteric acid, Dotarem®) was administered intravenously at a dose of 0.2 mL/kg using a 22-gauge

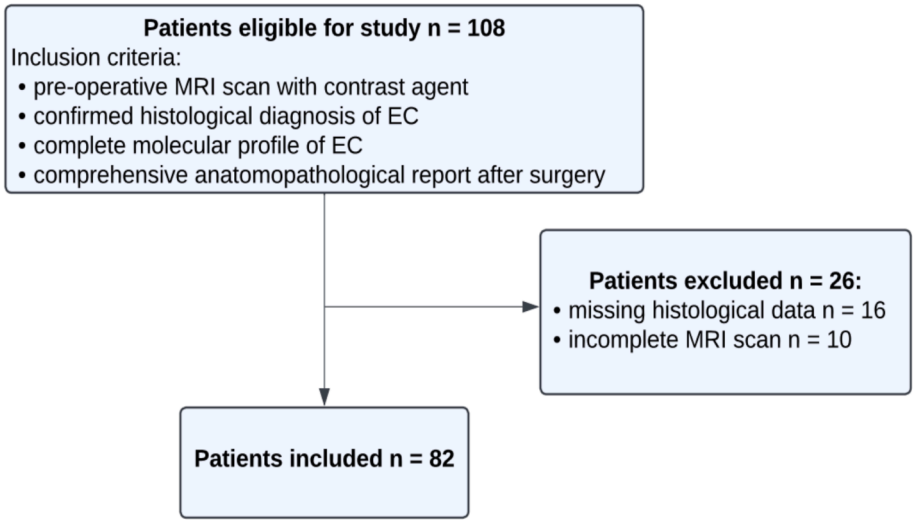

Fig. 1. Patient Inclusion and Exclusion Flowchart Criteria.

peripheral venous line and a power injector at 2 mL/s, followed by a 20 mL saline flush. Post-contrast images were captured at intervals of 6–10 s, beginning 10 s prior to the contrast injection, with a total imaging duration of 320 s.

2.4. Lymph Node analysis

LNs were retrospectively evaluated on MRI images according to Node-RADS guidelines [7]. The LN stations assessed included the common iliac, internal iliac, external iliac, and obturator. Each LN was categorized using Node-RADS, which assigns a risk category with a score ranging from 1 to 5, reflecting the suspicion of neoplastic involvement: '1-very low'; '2-low'; '3-equivocal'; '4-high'; and '5-very high.' The interpreting radiologist used a three-level flowchart for guidance. Levels 1 and 2 were centered on primary imaging criteria, specifically 'size' and 'configuration,' while level 3 provided the final Node-RADS score [Fig. 2].

Node-RADS assessments were performed independently by three readers with different levels of experience in pelvic MRI: a senior radiologist (LM) with 25 years of experience, and two junior radiologists with 2 and 4 years of experience (SR and RN), respectively. All readers were blinded to the histopathological reports [Fig. 3].

Finally, the diagnostic performance of Node-RADS score was evaluated in comparison to LN short-axis measurement alone.

2.5. Statistical analysis

Spearman's rank-order correlation test was performed to determine the correlation between the highest Node-RADS score assigned by the senior reader for each patient and pN status, as well as other clinical and radiological qualitative features (LVSI, aggressive tumors, histologic type, grade, pre- and post-operative FIGO stages, 2023 FIGO stage, myometrial invasion classified as < 50 % or > 50 %, presence of genetic mutations).

Additionally, the test was conducted to investigate the correlation between the configuration (in terms of texture, border, and shape according to Node-RADS, Fig. 2) of the LN to which the senior reader assigned the highest Node-RADS score and pN status. Furthermore, the correlation between the presence of genetic mutations and clinical and radiological qualitative features was assessed.

The Shapiro-Wilk test was used to determine whether quantitative features (e.g., age and lymph node short-axis diameter) followed a normal distribution. A one-way analysis of variance (ANOVA) was performed to evaluate if there were statistically significant differences in the quantitative features across the five Node-RADS score groups.

A receiver operating characteristic (ROC) curve was generated to calculate the area under the curve (AUC) and evaluate the diagnostic performance of the Node-RADS score for the three readers and lymph node short-axis diameter in predicting pN status. Sensitivity, specificity, PPV, NPV, and accuracy for the four possible Node-RADS score cutoffs (≥ 2, ≥ 3, ≥ 4, and 5) were calculated for the senior reader.

Cohen's κ was used to determine inter-reader agreement between Node-RADS scores assigned by the senior reader and those assigned by junior reader 1, as well as between the senior reader and junior reader 2, and between junior reader 1 and junior reader 2.

Statistical significance was set at $p < 0.05$. All data analyses were conducted using Statistical Package for the Social Sciences software (SPSS Statistics version 25.0, SPSS, Chicago, IL, USA).

3. Results

From our institutional database of 346 patients diagnosed with EC, we selected 108 patients who underwent preoperative pelvic MRI and surgery. Of these, 82 patients with histologically confirmed EC met the inclusion criteria and had their MRI images retrospectively reviewed. Twenty-six patients were excluded due to missing data, incomplete preoperative MRI, or disease progression.

The mean age was 64 years (range 36–87 years). Among the included patients, 68/82 (82.9 %) had no LNI on definitive histologic examination ($pN = 0$), while 14/82 (17.1 %) had at least one positive LN ($pN \geq 1$) in one of the eight evaluated pelvic LN stations.

The senior reader assigned Node-RADS scores of 1, 2, 3, 4, and 5 to 26/82 (31.7 %), 28/82 (34.1 %), 19/82 (23.2 %), 6/82 (7.3 %), and 3/82 (3.7 %) patients, respectively. The mean short-axis diameter of the lymph nodes to which the senior reader assigned the highest Node-RADS score was 8.2 mm (range: 4–22 mm).

Inter-observer agreements for Node-RADS scores between the senior reader and junior reader 1, between the senior reader and junior reader 2, and between junior reader 1 and junior reader 2 were 0.86 (95 % CI, 0.735 to 0.985, $p < 0.001$), 0.7 (95 % CI, 0.61 to 0.79, $p < 0.001$), and 0.7 (95 % CI, 0.577 to 0.823, $p < 0.001$), respectively.

A positive and significant correlation was found between the Node-RADS score and pN status ($rs = 0.451$, $p < 0.001$), pre-operative FIGO stage ($rs = 0.348$, $p = 0.001$), post-operative FIGO stage ($rs = 0.327$, $p = 0.003$), 2023 FIGO stage ($rs = 0.330$, $p = 0.002$), myometrial invasion ($rs = 0.288$, $p = 0.002$), and LVSI ($rs = 0.271$, $p = 0.014$).

Furthermore, a positive and significant correlation was found between LN configuration criteria and pN status (texture: $rs = 0.633$, $p <$

Table 1
Clinical, pathological and MRI qualitative characteristics of the study population.

			NODE-RADS						p-value
			1	2	3	4	5	Total	
Myometrial invasion	**<50 %**	N	19	21	10	2	19	21	**0.009**
		%	23.2 %	25.6 %	12.2 %	2.4 %	23.2 %	25.6 %	
	>50 %	N	7	7	9	4	7	7	
		%	8.5 %	8.5 %	11.0 %	4.9 %	8.5 %	8.5 %	
Pre-operative FIGO Stage	**IA**	N	16	15	9	1	0	41	**0.001**
		%	19.5 %	18.3 %	11.0 %	1.2 %	0.0 %	50.0 %	
	IA/B	N	1	0	0	0	0	1	
		%	1.2 %	0.0 %	0.0 %	0.0 %	0.0 %	1.2 %	
	IB	N	5	12	3	1	0	21	
		%	6.1 %	14.6 %	3.7 %	1.2 %	0.0 %	25.6 %	
	IB/IIIC1	N	0	0	1	1	0	2	
		%	0.0 %	0.0 %	1.2 %	1.2 %	0.0 %	2.4 %	
	II	N	0	1	1	1	0	3	
		%	0.0 %	1.2 %	1.2 %	1.2 %	0.0 %	3.7 %	
	IIIA	N	2	0	0	0	0	2	
		%	2.4 %	0.0 %	0.0 %	0.0 %	0.0 %	2.4 %	
	IIIB	N	1	0	0	0	0	1	
		%	1.2 %	0.0 %	0.0 %	0.0 %	0.0 %	1.2 %	
	IIIC1	N	1	0	3	1	1	6	
		%	1.2 %	0.0 %	3.7 %	1.2 %	1.2 %	7.3 %	
	IIIC2	N	0	0	2	0	1	3	
		%	0.0 %	0.0 %	2.4 %	0.0 %	1.2 %	3.7 %	
	IVB		0	0	0	1	1	2	
			0.0 %	0.0 %	0.0 %	1.2 %	1.2 %	2.4 %	
Post-operative FIGO Stage	**IA1**	N	17	19	7	2	0	45	**0.003**
		%	21.0 %	23.5 %	8.6 %	2.5 %	0.0 %	55.6 %	
	IA2	N	0	1	1	0	0	2	
		%	0.0 %	1.2 %	1.2 %	0.0 %	0.0 %	2.5 %	
	IB	N	2	6	7	0	0	15	
		%	2.5 %	7.4 %	8.6 %	0.0 %	0.0 %	18.5 %	
	II	N	2	1	1	2	0	6	
		%	2.5 %	1.2 %	1.2 %	2.5 %	0.0 %	7.4 %	
	IIIA	N	1	1	0	0	0	2	
		%	1.2 %	1.2 %	0.0 %	0.0 %	0.0 %	2.5 %	
	IIIB	N	1	0	0	0	0	1	
		%	1.2 %	0.0 %	0.0 %	0.0 %	0.0 %	1.2 %	
	IIIC1	N	1	0	0	1	0	2	
		%	1.2 %	0.0 %	0.0 %	1.2 %	0.0 %	2.5 %	
	IIIC2	N	0	0	1	0	2	3	
		%	0.0 %	0.0 %	1.2 %	0.0 %	2.5 %	3.7 %	
	IVB	N	1	0	2	1	1	5	
		%	1.2 %	0.0 %	2.5 %	1.2 %	1.2 %	6.2 %	
LVSI	**Negative**	N	18	27	10	1	1	57	**0.014**
		%	22.0 %	32.9 %	12.2 %	1.2 %	1.2 %	69.5 %	
	Positive	N	8	1	9	5	2	25	
		%	9.8 %	1.2 %	11.0 %	6.1 %	2.4 %	30.5 %	
Aggressive	**Negative**	N	18	24	13	3	2	60	0.576
		%	22.0 %	29.3 %	15.9 %	3.7 %	2.4 %	73.2 %	
	Positive	N	8	4	6	3	1	22	
		%	9.8 %	4.9 %	7.3 %	3.7 %	1.2 %	26.8 %	
Histological type	**Endometrioid**	N	23	27	16	4	3	73	0.367
		%	28.0 %	32.9 %	19.5 %	4.9 %	3.7 %	89.0 %	
	Carcinosarcomas	N	2	0	2	0	0	4	
		%	2.4 %	0.0 %	2.4 %	0.0 %	0.0 %	4.9 %	
	Clear cell adenocarcinomas	N	1	0	0	0	0	1	
		%	1.2 %	0.0 %	0.0 %	0.0 %	0.0 %	1.2 %	
	Serous adenocarcinomas	N	0	1	1	2	0	4	
		%	0.0 %	1.2 %	1.2 %	2.4 %	0.0 %	4.9 %	
Grade	**1**	N	4	9	3	0	0	16	0.240
		%	4.9 %	11.0 %	3.7 %	0.0 %	0.0 %	19.5 %	
	1–2	N	2	2	0	0	0	4	
		%	2.4 %	2.4 %	0.0 %	0.0 %	0.0 %	4.9 %	
	2	N	12	13	10	3	2	40	
		%	14.6 %	15.9 %	12.2 %	3.7 %	2.4 %	48.8 %	
	2–3	N	3	0	1	0	0	4	
		%	3.7 %	0.0 %	1.2 %	0.0 %	0.0 %	4.9 %	
	3	N	5	4	5	3	1	18	
		%	6.1 %	4.9 %	6.1 %	3.7 %	1.2 %	22.0 %	
pN Status	**0**	N	24	28	14	2	0	68	**< 0.001**
		%	29.3 %	34.1 %	17.1 %	2.4 %	0.0 %	82.9 %	
	≥1	N	2	0	5	4	3	14	
		%	2.4 %	0.0 %	6.1 %	4.9 %	3.7 %	17.1 %	

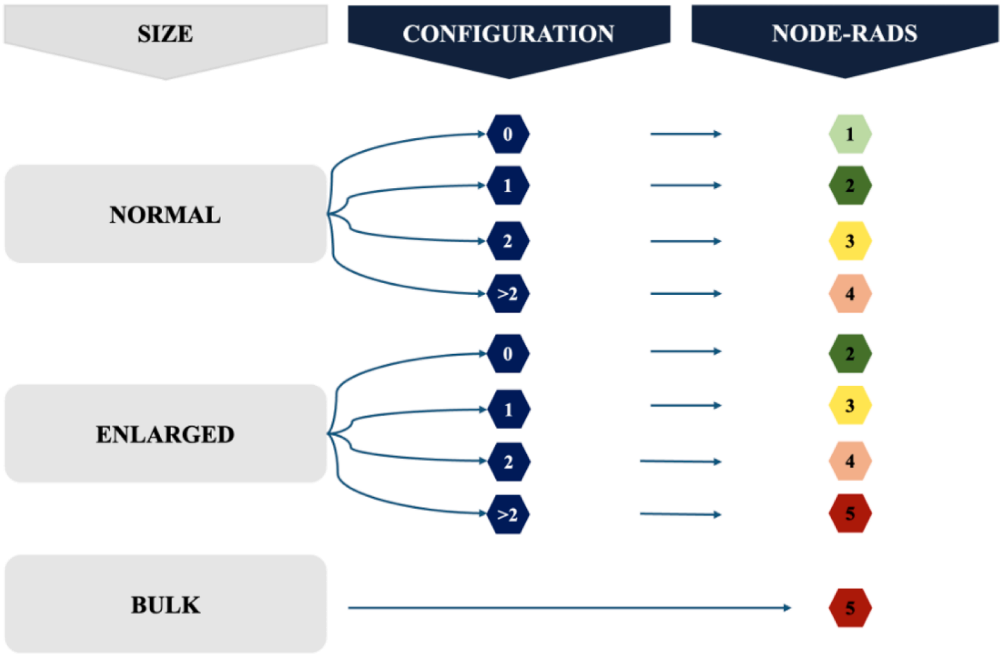

Size: choose one category			**Configuration:** choose one feature per category		
Normal: short axis	**Enlarged**: short axis	**Bulk**: any axis	**Texture**	**Border**	**Shape**
General: < 10 mm Inguinal: < 15 mm Facial, parotid, retroauricular, occipital, retropharyngeal, anterior jugular: < 5 mm Cardiophrenic, retrocrural, obturator, mesorectal: < 5 mm	Larger than normal, but not bulk ≥ 2 mm increase to prior imaging, if available	≥ 30 mm	Homogeneous: **0** Heterogeneous: **1** Focal necrosis: **2** Gross necrosis or any new necrosis: **3** Entity-specific findings *: **3**	Smooth: **0** Irregular or ill-defined: **1**	Any shape with preserved fatty hilum: **0** Kidney-bean-like or oval without fatty hilum: **0** Spherical without fatty hilum: **1**

Fig. 2. Node-RADS scoring system flowchart description criteria, adapted from the original publication.

0.001; border: rs = 0.351, p = 0.001; shape: rs = 0.494, p < 0.001).

Additionally, a significant positive correlation was observed between p53abn and post-operative FIGO stage (rs = 0.239, p = 0.014), histotype (rs = 0.451, p < 0.001), grade (rs = 0.357, p = 0.001), 2023 FIGO stage (rs = 0.398, p < 0.001), and aggressive tumors (rs = 0.406, p < 0.001).

The ANOVA test found a significant difference in LN short-axis diameter among the five Node-RADS score groups (F = 15.923, p < 0.001) but no significant difference in age (F = 1.349, p = 0.260).

Using Node-RADS scores, the prediction of pN status corresponded to an AUC of 0.832 for the senior reader, 0.807 for junior reader 1, and 0.802 for junior reader 2 [Fig. 4]. Using LN short-axis diameter alone, the prediction of pN status corresponded to an AUC of 0.704. The performance of the Node-RADS score assigned by the senior reader in predicting pN status in EC is shown in Table 2 [Table 2].

4. Discussion

LNI in patients with EC remains a crucial aspect of staging, as it influences therapeutic management. Current guidelines advocate for a selective approach to lymphadenectomy in EC, emphasizing the role of SLNB for staging in patients with presumed uterus-confined disease[16]. In cases where SLN is not detected, ESGO guidelines, recommend side-specific systematic lymphadenectomy in high-intermediate and high-risk patients, while it can be considered in presumed intermediate-risk cases[17]. This approach reduces unnecessary lymphadenectomy in low-risk cases, minimizing complications such as vascular injury, lymphedema, and lymphocele formation. SLNB involves injecting a tracer into the uterine cervix to identify the sentinel nodes, which are the first LNs to receive drainage from the tumor. A negative sentinel node is accepted to confirm pN0. This approach has demonstrated potential in reducing the morbidity linked to lymphadenectomy while preserving accurate staging[18,19].

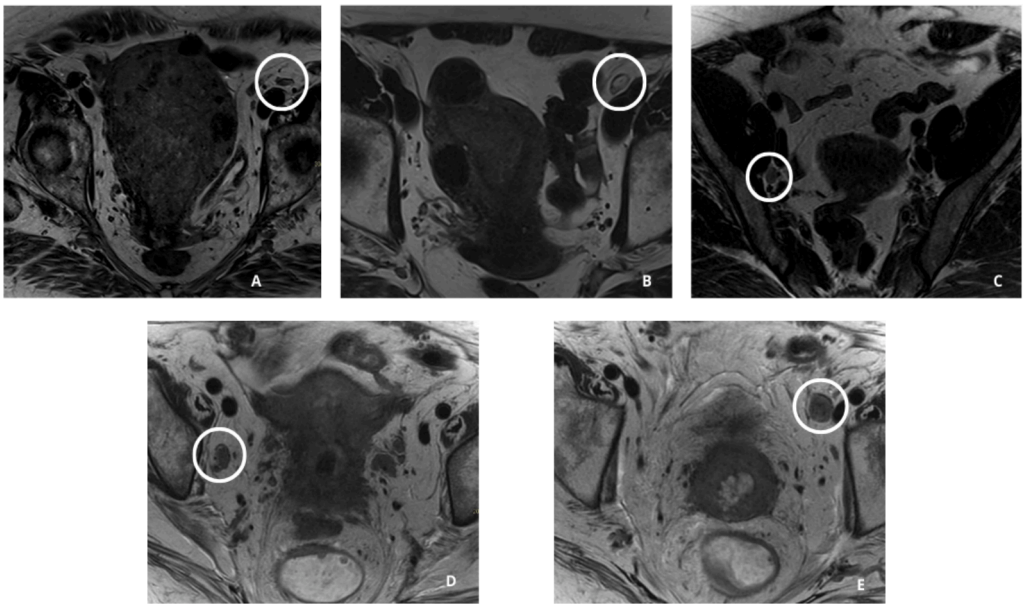

Fig. 3. Axial T2-weighted MRI sequences of endometrial cancer patients showcasing pelvic lymph nodes with different Node-RADS scores. **a** Node- RADS 1: left external iliac LN with normal size and configuration. **b** Node-RADS 2: left external iliac LN showing a short axis of 5 mm and homogeneous signal intensity and fatty hilum. **c** Node-RADS 3: the right external iliac LN showing a short axis of 8 mm, spherical without fatty hilum, heterogenous signal intensity. **d.** Node-RADS 4: right obturator LN, 10 mm of short axis, heterogenous texture, irregular border. **e.** Node-RADS 5: left external iliac LN, 13 mm of short axis, spherical without fatty hilum with focal necrosis.

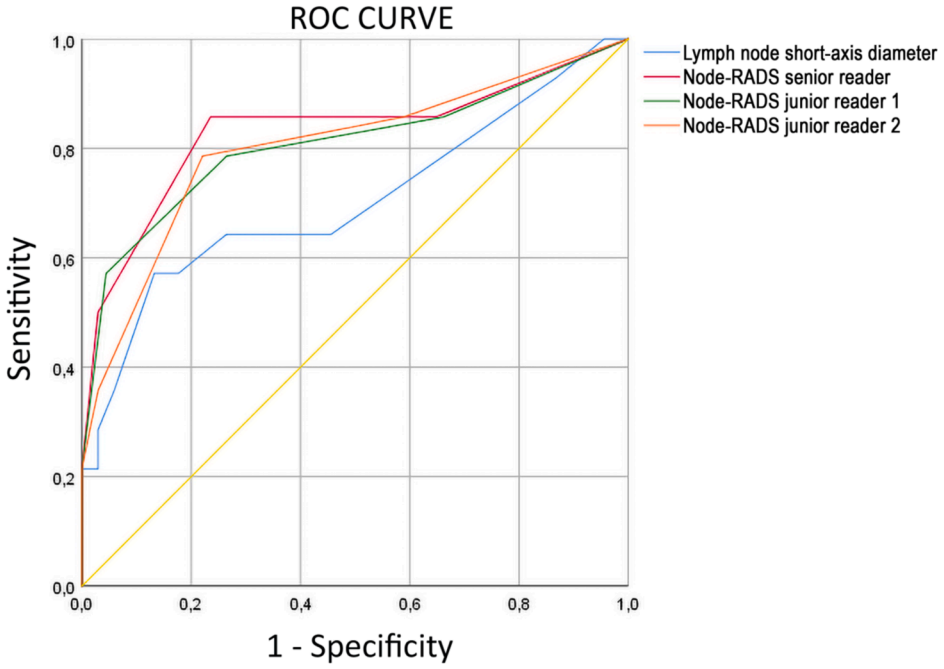

Fig. 4. Receiver operating characteristic (ROC) curve for the prediction of pN status. Area under the curve (AUC) = Lymph node short-axis diameter: 0.704; Node-RADS according to the senior reader: 0.832; Node-RADS according to junior reader 1: 0.807; Node-RADS according to junior reader 2: 0.802.

Table 2
Node-RADS score performance in predicting pN status in endometrial cancer.

Node-RADS Cutoff	Sensitivity (95 % CI)	Specificity (95 % CI)	PPV (95 % CI)	NPV (95 % CI)	Accuracy (95 % CI)
≥2	85.71 % (57.19–98.22 %)	35.29 % (24.08–47.83 %)	21.43 % (17.14–26.45 %)	92.31 % (76.17–97.83 %)	43.90 % (32.96–55.30 %)
≥3	85.71 % (57.19–98.22 %)	76.47 % (64.62–85.91 %)	42.86 % (31.72–54.77 %)	96.30 % (87.74–98.95 %)	78.05 % (67.54–86.44 %)
≥4	50.00 % (23.04–76.96 %)	97.06 % (89.78–99.64 %)	77.78 % (44.78–93.79 %)	90.41 % (84.79–94.10 %)	89.02 % (80.18–94.86 %)
5	21.43 % (4.66–50.80 %)	100.00 % (94.56–100.00 %)	100.00 % (29.24–100.00 %)	85.71 % (82.03–88.75 %)	86.25 % (76.73–92.93 %)

Different imaging techniques have been developed to assess LNI.

Ultrasound (US) is a non-invasive and cost-effective imaging modality, but it is limited to assessing superficial LNs and is highly operator dependent. A systematic review and *meta*-analysis by Borges et al. evaluated the diagnostic performance of transvaginal sonography (TVS) in the preoperative assessment of LN metastasis in gynecological cancers [20]. The study reported a sensitivity of 41 %, specificity of 98 %, and a diagnostic odds ratio of 32. Comparing these results with our study, using a Node-RADS score cutoff of ≥ 3, we found a lower specificity (98 % vs. 76.47 %) but a significantly higher sensitivity (41 % vs. 85.71 %). These findings suggest that Node-RADS may offer better detection of LN metastases at the expense of a slight reduction in specificity.

In the realm of advanced imaging, positron emission tomography/computed tomography (PET/CT) has gained recognition as a valuable tool in detecting LN metastasis in EC. Studies, such as the one conducted by Budak E, Yanarateş A. et al have shown that with regard to detecting LN metastasis, PET/CT exhibits high accuracy, sensitivity, and specificity, with reported values of 95 %, 80 %, and 96 %, respectively, for detecting LN metastasis[21–23]. Despite its promising performance, PET/CT has drawbacks, such as high costs, limited availability, and the radiation exposure involved, which may limit its routine use. Additionally, PET/CT has reduced sensitivity in detecting small metastatic lesions, and its non-specific uptake can lead to overstaging, thus complicating treatment planning.

In this context, there is a need to investigate an accurate LN assessment that can guide patients toward less invasive diagnostic procedures.

Pelvic MRI has proven to be an effective non-invasive imaging technique for assessing LNI in EC as it provides detailed information on local tumor spread, including myometrial invasion, cervical invasion, parametrial involvement, and nearby tissue involvement, which are crucial factors in staging and treatment planning. MRI's ability to offer a comprehensive anatomical assessment helps to determine whether lymphadenectomy or SLNB is necessary, making it a valuable tool in preoperative planning.

This study highlights a significant correlation between the Node-RADS score and histologically confirmed LNI, with an AUC of 0.832. This suggests that Node-RADS may serve as a reliable tool for assessing LN metastasis in EC. The Node-RADS score demonstrated high sensitivity, and Node-RADS levels of ≥ 4 and 5 showed excellent specificity and PPV.

Accurate identification of LN that are free from metastases is essential to prevent the inadvertent retention of malignant LNs during surgical resection, which could facilitate further cancer spread. Therefore, the NPV should be as high as possible, exceeding the values provided by the Node-RADS cutoffs of ≥ 4 and 5, which were 90.41 % (84.79 %–94.10 %) and 85.71 % (82.03 %–88.75 %), respectively.

Based on our findings, we identified Node-RADS ≥ 3 as the optimal cutoff in detecting pathological lymph nodes, achieving an accuracy of 76.83 % and a NPV of 96.30 % (87.74 %–98.95 %).

While this cut off slightly lowers specificity from 100 % (for Node-RADS 5) to 76.47 %, it significantly improves sensitivity from 21.43 % to 78.57 %. These results align with previous studies showing that a Node-RADS score of ≥ 3 is an optimal cut off in detecting LNI among multiple cancer types.

Node-RADS scores of ≥ 3 have also been validated as optimal cutoffs in cervical cancer, exhibiting a sensitivity of 92.86 %, specificity of 72.5 %, and a NPV of 93.55 %. The same cutoff values have yielded consistent results also in colon, rectal, and prostate cancers[9,11,12,8].

A systematic review by Jingyu Zhong et al. found that both Node-RADS ≥ 3 and Node-RADS ≥ 4 show strong diagnostic accuracy. However, Node-RADS ≥ 3 offers higher specificity at a slight cost to sensitivity. Thus, it may be the optimal cutoff in the absence of specific clinical indications, aligning with our findings [24].

This consistency among various cancers highlights the potential utility of Node-RADS as a standard metric in cancer staging.

In fact, the criteria for LNI remain a challenge. Currently, the short-axis diameter measured on the axial plane is the most widely used criterion for assessing LNI. However, this study demonstrates that the Node-RADS score could improve diagnostic performance, achieving a higher AUC compared to the short-axis diameter alone (AUC = 0.832 vs. AUC = 0.704). This improvement may be attributed to the incorporation of both size and morphological criteria within the Node-RADS score, as evidenced by the significant correlation between configuration criteria (texture, border, and shape) and pathologically confirmed nodal status ($p < 0.001$).

Furthermore, the inter-observer agreement for Node-RADS scores was high, with κ values of 0.86 and 0.7 between senior and junior readers, indicating that Node-RADS is reproducible among different levels of expertise.

In 2023, Berek JS, Matias-Guiu X, et al. updated the FIGO staging system for EC to include molecular markers, histological subtypes, grading, and LVSI[3]. Our study further explored the impact of these revised FIGO 2023 criteria on Node-RADS scoring. We found a positive correlation between the Node-RADS score, myometrial invasion, and LVSI, suggesting that these new criteria can enhance the accuracy of LN assessments when combined with Node-RADS.

A significant association was identified between p53 mutations, tumor grade, and aggressive histological subtypes, consistent with TCGA data, which links POLEmut with favorable prognosis and p53abn with poorer outcomes. However, no correlation was found between p53abn and the Node-RADS score. This could be explained by the fact that some tumors, while highly aggressive due to p53 mutations, do not necessarily exhibit lymphatic spread. The p53 mutation, while associated with poor prognosis and high tumor grade, may not always predict nodal metastasis, as certain aggressive tumors tend to grow locally rather than spreading through the lymphatic system. This observation emphasizes the complexity of tumor biology and the need for a multifactorial approach to assess both local and distant metastasis risks in EC.

These findings suggest that Node-RADS can serve as a complementary tool to be included in the structured report based on the updated FIGO staging system, providing a more comprehensive assessment of LNI. The incidence of LN metastasis in EC varies by tumor stage and grade. While low-grade, minimally invasive tumors have a metastasis rate of 3–5 %, high-grade tumors with deep myometrial invasion exceed a 20 % incidence rate of LNI [25].

Our study population, with a mean age of 64 years, reflects typical demographic characteristics of EC patients, aligning with known incidence trends. These findings contribute to the ongoing efforts to refine staging and management in EC, stressing the importance of incorporating both molecular and imaging-based assessments into clinical decision-making.

However, our study has some limitations. The retrospective design of this study introduces potential bias. Firstly, it may lead to an overestimation of diagnostic accuracy, since only patients with a confirmed disease status are included. Additionally, the selection of specific patients limits the generalizability of the findings, making them less applicable to a broader patient population.

Therefore, further research with larger patient cohorts is necessary to standardize and validate our findings. Secondly, the assessments were conducted by radiologists experienced in gynecological oncological imaging, which could limit the applicability of the scoring system on a global scale. Lastly, not all histological analyses and molecular profiles are routinely available in clinical practice, potentially affecting the broader application of our results.

Conversely, the inter-reader agreement was found to range from good to excellent, even among radiologists with less experience in gynecological imaging. This high level of concordance highlights the potential applicability of the Node-RADS scoring system, supporting its integration into clinical practice and structured reporting.

This study highlighted that imaging, particularly MRI, serves as a complementary tool to pathological anatomy in the staging of EC, especially for assessing LNI.

To further enhance the applicability of the Node-RADS score, additional studies should be conducted, including multicenter trials with larger and more different patient cohorts. These studies should not only aim to validate and standardize the findings among different institutions but also thoroughly explore the potential application of the Node-RADS score in various imaging modalities, such as CT. However, it is important to note that CT evaluation is not systematically performed in low-risk EC.

Consequently, the validation of Node-RADS may be influenced by selection bias, leading to a patient cohort that is not fully representative of the broader EC population. Moreover, incorporating key clinical parameters, into Node-RADS such as patient age, tumor size, LVSI, and histopathological characteristics, may enhance the accuracy of LN involvement assessment for EC patients. Additionally, qualitative MRI features, including DWI and ADC mapping, have demonstrated potential in improving the diagnostic performance of LN characterization and could be incorporated into Node-RADS. A comprehensive evaluation of its performance among different modalities would provide critical insights into its diagnostic accuracy, versatility, and broader clinical utility, facilitating its integration into routine practice and standardized reporting in gynecologic oncology.

5. Conclusion

Node-RADS represents a valuable imaging tool for the assessment of LNI in patients with EC. By incorporating both size and morphological characteristics of LN, it has demonstrated a significant correlation with histopathologically confirmed LNI.

Furthermore, Node-RADS shows potential as a non-invasive approach to guide clinical decision-making regarding the necessity of systematic lymphadenectomy, thereby facilitating a more accurate preoperative evaluation of lymphatic spread. The high interobserver reproducibility of the system, regardless of the radiologist's level of experience, further underscores its reliability and clinical applicability.

This study also emphasizes the importance of integrating imaging-based tools such as Node-RADS with the updated molecular and histological classifications introduced in the 2023 FIGO staging system. Combining these advanced imaging techniques with molecular subclassification offers the potential to improve the precision of cancer staging and prognosis. Such an integrative approach could enable personalized treatment strategies, enhance patient outcomes, and minimize unnecessary surgical interventions.

Declaration of competing interest

The authors declare that they have no known competing financial interests or personal relationships that could have appeared to influence the work reported in this paper.

References

[1] Endometrial cancer statistics. World Cancer Research Fund. Accessed November 18, 2024. https://www.wcrf.org/preventing-cancer/cancer-statistics/endometrial-cancer-statistics/.

[2] E.J. Crosbie, S.J. Kitson, J.N. McAlpine, A. Mukhopadhyay, M.E. Powell, N. Singh, Endometrial cancer, *Lancet.* 399 (10333) (2022) 1412–1428, https://doi.org/10.1016/S0140-6736(22)00323-3.

[3] J.S. Berek, X. Matias-Guiu, C. Creutzberg, et al., FIGO staging of endometrial cancer: 2023, *Int J Gynecol Obstet.* 162 (2) (2023) 383–394, https://doi.org/10.1002/ijgo.14923.

[4] Frost JA, Webster KE, Bryant A, Morrison J. Lymphadenectomy for the management of endometrial cancer - Frost, JA - 2017 | Cochrane Library. Accessed November 18, 202. https://www.cochranelibrary.com/cdsr/doi/10.1002/14651858.CD007585.pub4/full.

[5] Maheshwari E, Nougaret S, Stein EB, et al. Update on MRI in Evaluation and Treatment of Endometrial Cancer. *Radiogr Rev Publ Radiol Soc N Am Inc.* 2022;42 (7):2112-2130. doi:10.1148/rg.220070.

[6] K. Kinkel, R. Forstner, F.M. Danza, et al., Staging of endometrial cancer with MRI: Guidelines of the European Society of Urogenital Imaging, *Eur Radiol.* 19 (7) (2009) 1565–1574, https://doi.org/10.1007/s00330-009-1309-6.

[7] F.H.J. Elsholtz, P. Asbach, M. Haas, et al., Introducing the Node Reporting and Data System 1.0 (Node-RADS): a concept for standardized assessment of lymph nodes in cancer, *Eur Radiol.* 31(8):6116 (2021), https://doi.org/10.1007/s00330-020-07572-4.

[8] S. Lucciola, M.L. Pisciotti, M. Frisenda, et al., Predictive role of node-rads score in patients with prostate cancer candidates for radical prostatectomy with extended lymph node dissection: comparative analysis with validated nomograms, *Prostate Cancer Prostatic Dis.* 26 (2) (2023) 379–387, https://doi.org/10.1038/s41391-022-00564-z.

[9] R.V. Ninkova, A. Calabrese, F. Curti, et al., The performance of the node reporting and data system 1.0 (Node-RADS) and DWI-MRI in staging patients with cervical carcinoma according to the new FIGO classification (2018), *Radiol Med (torino)* 129 (7) (2024) 1062–1075, https://doi.org/10.1007/s11547-024-01824-9.

[10] C. Leonardo, R.S. Flammia, S. Lucciola, et al., Performance of Node-RADS Scoring System for a Standardized Assessment of Regional Lymph Nodes in Bladder Cancer Patients, *Cancers.* 15 (3) (2023) 580, https://doi.org/10.3390/cancers15030580.

[11] N. Maggialetti, C.N. Greco, N.M. Lucarelli, et al., Applications of new radiological scores: the Node-rads in colon cancer staging, *Radiol Med (torino).* 128 (11) (2023) 1287–1295, https://doi.org/10.1007/s11547-023-01703-9.

[12] Y. Niu, S. Yu, P. Chen, M. Tang, L. Wen, Y. Sun, Y. Yang, Y. Zhang, Y. Fu, Q. Lu, T. Luo, X. Yu, Diagnostic performance of Node-RADS score for mesorectal lymph node metastasis in rectal cancer, *Abdom Radiol* 50 (1) (2024) 38–48, https://doi.org/10.1007/s00261-024-04497-0.

[13] S. Nougaret, M. Horta, E. Sala, et al., Endometrial Cancer MRI staging: Updated Guidelines of the European Society of Urogenital Radiology, *Eur Radiol.* 29 (2) (2019) 792–805, https://doi.org/10.1007/s00330-018-5515-y.

[14] ESGO/ESTRO/ESP guidelines for the management of patients with endometrial carcinoma - PubMed. Accessed January 15, 2025. https://pubmed.ncbi.nlm.nih.gov/33397713/.

[15] M. Sbarra, M. Lupinelli, O.R. Brook, A.M. Venkatesan, S. Nougaret, Imaging of Endometrial Cancer, *Radiol Clin North Am.* 61 (4) (2023) 609–625, https://doi.org/10.1016/j.rcl.2023.02.007.

[16] A. Oaknin, T.J. Bosse, C.L. Creutzberg, et al., Endometrial cancer: ESMO Clinical Practice Guideline for diagnosis, treatment and follow-up, *Ann Oncol.* 33 (9) (2022) 860–877, https://doi.org/10.1016/j.annonc.2022.05.009.

[17] N. Concin, X. Matias-Guiu, I. Vergote, et al., ESGO/ESTRO/ESP guidelines for the management of patients with endometrial carcinoma, *Int J Gynecol Cancer off J Int Gynecol Cancer Soc.* 31 (1) (2021) 12–39, https://doi.org/10.1136/ijgc-2020-002230.

[18] G. Bogani, A. Papadia, A. Buda, et al., Sentinel node mapping vs. sentinel node mapping plus back-up lymphadenectomy in high-risk endometrial cancer patients: Results from a multi-institutional study, *Gynecol Oncol.* 161 (1) (2021) 122–129, https://doi.org/10.1016/j.ygyno.2021.01.008.

[19] G. Bogani, A. Giannini, E. Vizza, V. Di Donato, F. Raspagliesi, Sentinel node mapping in endometrial cancer, *J Gynecol Oncol.* 35 (1) (2024) e29.

[20] Borges AC, Veloso H, Galindo P, et al. OBGYN. doi:10.1002/uog.27633.

[21] A. Kilcoyne, D.Z. Chow, S.I. Lee, FDG-PET for Assessment of Endometrial and Vulvar Cancer, *Semin Nucl Med.* 49 (6) (2019) 471–483, https://doi.org/10.1053/j.semnuclmed.2019.06.011.

[22] C. Sallée, F. Margueritte, S. Gouy, et al., FDG-PET/CT and Para-Aortic Staging in Endometrial Cancer. A French Multicentric Study, *J Clin Med.* 10(8):1746 (2021), https://doi.org/10.3390/jcm10081746.

[23] E. Budak, A. Yanarateş, The value of PET/CT in determining lymph node metastasis of endometrial cancer, *Ginekol Pol.* 90 (10) (2019) 565–570, https://doi.org/10.5603/GP.2019.0098.

[24] Zhong J, Mao S, Chen H, et al. Node-RADS: a systematic review and meta-analysis of diagnostic performance, category-wise malignancy rates, and inter-observer reliability. *Eur Radiol.* Published online November 6, 2024. doi:10.1007/s00330-024-11160-1.

[25] C. Nahshon, Y. Kadan, O. Lavie, L. Ostrovsky, Y. Segev, Sentinel lymph node sampling versus full lymphadenectomy in endometrial cancer: a SEER database analysis, *Int J Gynecol Cancer off J Int Gynecol Cancer Soc.* 33 (10) (2023) 1557–1563, https://doi.org/10.1136/ijgc-2023-004474.